Water Research 147 (2018) 13–24

Contents lists available at ScienceDirect

Water Research

journal homepage: www.elsevier.com/locate/watres

# Large greenhouse gases emissions from China's lakes and reservoirs

Siyue Li [a, *], Richard T. Bush [b], Isaac R. Santos [c], Quanfa Zhang [d], Kaishan Song [e], Rong Mao [a], Zhidan Wen [e], Xi Xi Lu [f, g]

[a] Research Center for Eco-hydrology, Chongqing Institute of Green and Intelligent Technology, The Chinese Academy of Sciences, Chongqing, 400714, China
[b] International Centre for Balanced Land Use, Newcastle Institute for Energy & Resources, The University of Newcastle, NSW, 2308, Australia
[c] National Marine Science Centre, Southern Cross University, Coffs Harbour, NSW, 2450, Australia
[d] Key Laboratory of Aquatic Botany and Watershed Ecology, Wuhan Botanical Garden, The Chinese Academy of Sciences, Wuhan, 430074, China
[e] Northeast Institute of Geography and Agroecology, The Chinese Academy of Sciences, Changchun, 130102, China
[f] Department of Geography, National University of Singapore, 119260, Singapore
[g] College of Ecology and Environment, University of Inner Mongolia, 010021, China

ARTICLE INFO

*Article history:*
Received 26 April 2018
Received in revised form
7 August 2018
Accepted 26 September 2018
Available online 29 September 2018

*Keywords:*
Carbon emission
Methane evasion
Reservoir
Lakes
Global climate change
Carbon cycle

ABSTRACT

Freshwaters are important sources of greenhouse gases (GHGs) to the atmosphere that may partially offset the terrestrial carbon sink. However, current emission estimates from inland waters remain uncertain due to data paucity in key regions with a large freshwater surface area, such as China. Here, we show that the areal fluxes of GHGs (carbon dioxide, methane, and nitrous oxide) from lakes and reservoirs in China are much larger than previous estimates. Our work summarized data from 310 lakes and 153 reservoirs, and revealed diffusive emissions of 1.56 (95% confidence interval: 1.12–2.00) Tg C-$CH_4$/y and 25.2 (20.8–29.5) Tg C-$CO_2$/y from reservoirs and lakes. Chinese lakes and reservoirs emit 175.0 (134.7–215.3) Tg $CO_2$ equivalent, with 73.4% of this forcing contributed by lakes. These aquatic sources are equivalent to 14.1%–22.6% of China's estimated terrestrial carbon sink. Our results suggest a disproportionally high contribution of China's reservoirs and lakes to national and global GHGs emissions, highlighting major data gaps and the need of including more artificial and natural lakes data from developing countries like China in global GHGs budgets.



## 1. Introduction

Natural lakes and artificial reservoirs, two major inland water ecosystems, are recognized as significant sources of greenhouse gases (GHGs) like methane ($CH_4$), carbon dioxide ($CO_2$) and nitrous oxide ($N_2O$) to the atmosphere (St Louis et al., 2000; Cole et al., 2007; Aufdenkampe et al., 2011; Barros et al., 2011; Bastviken et al., 2011; Raymond et al., 2013; Deemer et al., 2016). Previous estimates indicated a total global emission from temperate regions of 23.7 Tg C-$CH_4$ from lakes (3.6 Tg C-$CH_4$ as diffusion-driven), 0.53 Tg C-$CH_4$ from reservoirs, and 80 Tg C-$CO_2$ from lakes and reservoirs surfaces per year (Bastviken et al., 2004, 2011; Aufdenkampe et al., 2011). The true GHGs fluxes may be larger. Additional and potentially significant emission pathways such as dam spillways and turbines, and downstream emissions below dams are difficult to quantify (Hertwich, 2013; Deemer et al., 2016). Despite of high uncertainties, emission from lakes and reservoirs may offset a significant fraction of the global terrestrial net carbon (C) sink (Aufdenkampe et al., 2011; Bastviken et al., 2011).

The global picture on GHGs flux estimates from inland waters is limited by uncertainties in key, large, developing countries such as China where hydroelectric dams are being constructed at a rapid rate (Zarfl et al., 2015). As a result of large GHGs emissions, the “green” credentials of hydroelectric reservoirs have been questioned (Giles, 2006; Barros et al., 2011). Reservoir emissions may partially offset fossil-fuel savings related to hydropower consumption in temperate and tropical areas where a majority of reservoirs are located (dos Santos et al., 2006; Bastviken et al., 2011).

Despite widespread evidence of substantial GHGs emissions from lakes and reservoirs on a local, regional and global scale (Tranvik et al., 2009; Bastviken et al., 2011; Raymond et al., 2013; Li and Zhang, 2014a; Li and Bush, 2015), estimates remain uncertain because of data scarcity. It is important to improve regional estimates, especially in developing countries where datasets are often

* Corresponding author.
*E-mail address:* syli2006@163.com (S. Li).

https://doi.org/10.1016/j.watres.2018.09.053
0043-1354/

less detailed. Indeed, previous observations were primarily made in European and North American waterbodies. Limited datasets are available from large developing countries like India and China, where the areal GHG fluxes from inland waters may be highly different than European and North American systems (Yang et al., 2011a). Large scale extrapolation from field data in Europe and North America thus may result in large uncertainty of the global carbon budget. Here, we focus on China, where a large expanse of freshwater areas exists.

China now possesses half of the world's total number of dams, and has the largest amount of hydropower generation capacity (1100 billion kWh, 27.5% of the world's total) (MWR, 2016; NEA, 2016). China had ~40 small reservoirs in the year of the foundation of the People's Republic of China in 1949. Dam construction in China experienced a rapid growth in the two decades of the 1950s and 1960s when the number of dams rose remarkably to 72,000. The number of reservoirs in China slowly increased after the 1980s, and rose to 98,000 in 2015 (MWR, 2016). The annual increase of the total reservoir storage capacity of the nation was the greatest rate after 2000 because of the completion of massive reservoirs such as the Three Gorges Dam (Yang and Lu, 2013). The boom in reservoir construction is a result of multiple demands, such as flood control, more stable water supplies, and energy demand. In 2011, China vowed to update the country's water infrastructures to alleviate water scarcity and provide cleaner energy. As a result, dam construction has been drastically accelerated with hydropower generation capacity nearly doubled between 2010 (ca. 216 GW) and 2020 (ca. 380 GW) and a related increase in reservoir surface area (NEA, 2016). Little is known on how these dam constructions will alter GHGs emissions from inland waters.

Here, we estimate for the first time diffusive emissions of methane and carbon dioxide from reservoirs and lakes, using available data from 310 lakes and 153 reservoirs across China (Fig. 1). China has a freshwater area of 26,870 $km^2$ for reservoirs and 82,232 $km^2$ for lakes (Yang and Lu, 2013), representing 23% of reservoir and 6.2% of lake areas between 25° and 54° latitude worldwide (Downing et al., 2006, 2012; Bastviken et al., 2011; Verpoorter et al., 2014). We provide a comprehensive assessment of GHGs emissions from China's lakes and reservoirs, their contribution to global GHGs budgets, variability within systems (i.e., pelagic versus littoral zones), and insight into the contribution from China's five major geographical zones (Fig. 1).

## 2. Methods

### 2.1. Site description

We geographically divided lakes into five regions in China: East Plain lakes zone (EPL), Qinghai-Tibetan Plateau lakes zone (TPL), Inner Mongolia-Xinjiang lakes zone (IMXL), Northeast Plain and Mountain lakes zone (NPML), and Yunnan-Guizhou Plateau lakes zone (YGPL). The TPL, EPL, IMXL lakes, respectively, represent 50%, 25% and 15% of China's lake area, and thus the three main lakes regions contribute 90% to the total lake area (82,232 $km^2$) of China. The NPML and YGPL lakes account for approximately 8.5% and 1.5% of China's lake area, respectively (Ma et al., 2011; Yang and Lu, 2013). Reservoirs cover an area of 26,870 $km^2$ and constitute 0.28% of the territorial land surface of China (Yang and Lu, 2013).

Combining lakes with reservoirs provides a total water area of 109,102 $km^2$, comprising 1.14% of China's territorial land surface. This percentage is much smaller than the global average of ~3.7% (Verpoorter et al., 2014), but the contribution of reservoirs to the total land area in China (0.28%) is much higher than the global average (0.18%). More importantly, China's lakes and reservoirs constitute 6.2% and 23.0% of the water surface area of the respective lakes and reservoirs in the temperate zone (Bastviken et al., 2011).

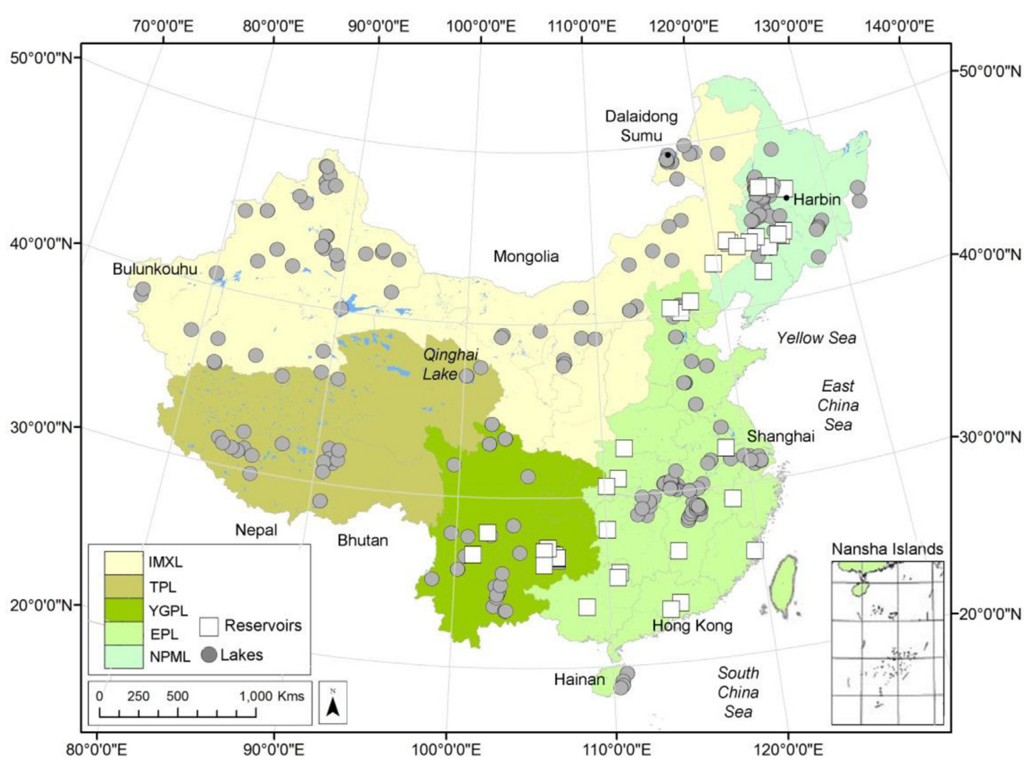


**Fig. 1.** China's map highlighting reservoirs and lakes with available data in the five geographic lake zones across mainland China. (1) The Tibetan Plateau Lake Zone (TPL); (2) The Eastern Plain Lake Region (EPL); (3) The Inner Mongolia-Xinjiang Lake Zone (IMXL); (4) The Northeast Plain and Mountain Lake Zone (NPML); (5) The Yunnan-Guizhou Plateau Lake Zone (YGPL). 50% of lake area is in TPL, 25% in the EPL, 15% in the IMXL, 8.5% in the NPML and 1.5% in the YGPL.

The sizes of our collected lakes range from 0.01 to 4380 $km^2$, and surfaces of reservoirs are from 0.02 to 1080 $km^2$. Size distribution and abundance of lakes and impoundments were assessed in 7 size categories (DelSontro et al., 2018). Data proportions from lakes with areas between 0.001 and 0.01, 0.01–0.1, 0.1–1, 1–10, 10–100, 100–1000 and 1000–10000, were 0.2%, 0, 4.9%, 13.7%, 29.8%, 36.5% and 14.8%, respectively. Data proportions for reservoirs covering the same 7 size categories were respectively 0, 0, 3.6%, 20.6%, 22.2%, 4.0% and 49.6%. Overall, size distribution of lakes and reservoirs with large area had more sampling data (Yang and Lu, 2013) (more information please refer to supplementary material).

### *2.2. Data collection*

We collated data for diffusion-driven $CH_4$, $CO_2$ and $N_2O$ emissions in reservoirs and lakes from the literature, complemented with some unpublished studies (Supplementary Tables S1 and S2). In total, we assembled 627 observations of GHGs areal fluxes from lakes and 293 estimates from reservoirs. Nitrous oxide data (45 estimates for reservoirs and 116 for lakes) were also included wherever they are available (Supplementary Tables S1 and S2). Methane and $N_2O$ areal fluxes were consistently measured using gas chromatography (GC) and floating chambers or headspace technique. $CO_2$ data was either directly determined using GC with chambers and headspace technique or derived from pH, alkalinity and temperature using $CO_2$sys (detailed information on supplementary material).

$CH_4$ and $CO_2$ areal fluxes from around additional 91 lentic systems in North China (15 reservoirs in North China, 63 lakes in NPML, and 13 lakes in IMXL) were determined using headspace equilibrium method (these data are marked “unpublished data” in the supplementary excel file). 2–26 samples were taken from individual lake or reservoir in the year of 2013–2014. Nutrients and organic carbon were also measured.

Additional field investigations were performed in lakes in YGPL and EPL in October 2015 and July–September 2017 to compare the three main methods (floating chamber with GC, thin boundary layer model (TBL) from headspace with GC and TBL from alkalinity and pH), which were used for comparative assessment of different methods. A total of 79 samples were taken, and carbon and nutrients were also determined.

Water chemistry (pH, carbon and nutrients), physical characteristics (geographic coordinates, age, mean depth, volume and area) and climate (air and water temperature and rainfall) were extracted for all reservoir and lake systems (Supplementary Tables S1 and S2). Reservoir and lake areas and volume were calculated using remote sensing images with ArcGIS (Ma et al., 2011; Yang and Lu, 2013). Landsat Thematic Mapper (TM) and Enhanced Thematic Mapper Plus (ETM+) with 30 m spatial resolution were used, and these TM/ETM + images are mainly acquired after the monsoon season (September–October) in the period 2005 to 2008. The statistical areas include reservoirs and lakes with surfaces greater than 0.0036 $km^2$. The surfaces of lakes with flux data are larger than 0.01 $km^2$. Lakes with an area less than 0.01 $km^2$ have a cumulative surface area of 540 $km^2$, accounting for approximately 0.66% of total lake surface area, and reservoirs with an area less than 0.01 $km^2$ have a combined surface area of 144 $km^2$, accounting for 0.54% of total reservoir surface area in China (Yang and Lu, 2013). Thus, GHGs fluxes from these very small ponds could be negligible because of their minor contribution to total surfaces, albeit recent report demonstrated higher GHGs areal fluxes from small ponds (Holgerson and Raymond, 2016). $CO_2$ equivalents are a widely-recognized tool for comparing GHGs. The total GHG footprints were calculated by converting $CH_4$ and $N_2O$ emissions to $CO_2$ equivalents and summing with the $CO_2$ emission results (Myhre et al., 2013).

We supplied detailed information on data quality control, water-air interface GHGs areal fluxes calculations and uncertainty analyses in the supplementary material. We here highlighted the key parameter pH for $CO_2$ fluxes uncertainty. Samples for $CO_2$ fluxes estimated from pH and alkalinity had pH average of $8.12 \pm 0.40$ (median 8.20 with quartiles of 7.90–8.40) ($n = 79$) for reservoirs, while pH in lakes averaged $8.40 \pm 0.86$ with a median of 8.26 (quartiles: 7.83–9.02) ($n = 255$). Thus, overestimation of calculated $CO_2$ areal flux from pH and alkalinity is likely to be minor (Abril et al., 2015).

### *2.3. Statistical analyses*

Relationships between GHGs fluxes and physicochemical variables were examined by means of linear and exponential regressions (Spearman's rho was also provided; see supplementary information). Variables with non-normal distribution were log-transformed to approach normality. For data sets containing negative gaseous fluxes (negative sign represents net carbon sink), we added a constant to get the regression model through log transformation. A constant of 1000 was added for reservoir $CO_2$ areal flux, 500 for lake $CO_2$, and 5 for lake $CH_4$. We used stepwise multiple regressions to identify which variables explained the variance in $CO_2$, and $CH_4$ emission rates, and used $p < 0.05$ for the significance probability for each control variable. However, a limited number of $N_2O$ emission rates prevented the use of regression analyses. All statistical analyses were carried out using SPSS 16.0 and SigmaPlot 11.0.95% confidence intervals (CI) were used to present uncertainties of estimates of GHGs fluxes.

We separated the waterbodies into categories of reservoirs and lakes. Reservoirs were further separated into pelagic and drawdown areas. Lakes were categorized into five geographic zones and pelagic and littoral areas (Fig. 1). Then national estimates were obtained by upscaling the average emissions for those categories.

## 3. Results

### *3.1. Reservoir GHGs emissions in China*

All of the sampled reservoirs were sources of $CH_4$ and $N_2O$ to the atmosphere via diffusive emissions, and 74% of the sampled reservoirs were sources of $CO_2$. The reservoirs that were sinks of $CO_2$ were only small sinks (0.3%–13.5% of the maximal $CO_2$ emission rate; $-586$ to $-12$ mg C-$CO_2$/$m^2$/d) in the pelagic zone (Figs. 2 and 3; Supplementary Table S3). The reservoirs had a wide range of gas exchange rates as net sources from near zero to a maximum of 4354 mg C-$CO_2$/$m^2$/d, 359 mg C-$CH_4$/$m^2$/d and 7.11 mg N-$N_2O$/$m^2$/d (Fig. 3; Supplementary Table S3).

We report mean areal (per unit surface area) $CH_4$ flux ($10.25 \pm 33.37$ mg C-$CH_4$/$m^2$/d, 95% confidence interval (CI): 4.51–16.0 mg C-$CH_4$/$m^2$/d) from reservoir pelagic areas, approximately 12%–32% smaller than previous estimates in worldwide temperate reservoirs (Tables 1 and 2). $CO_2$ flux estimates ($532.5 \pm 781.7$ mg C-$CO_2$/$m^2$/d, 95% CI: 432.9–632.1 mg C-$CO_2$/$m^2$/d) were approximately 35% larger than the temperate average (Table 2), up to 1 order of magnitude higher than those measured in the same climate of Europe and USA (Halbedel and Koschorreck, 2013; Knoll et al., 2013), but similar to the global reservoir estimates (500 mg C-$CO_2$/$m^2$/d; Table 2). Our first estimate of reservoir $N_2O$ flux for China ($1.02 \pm 1.43$ mg N-$N_2O$/$m^2$/d, 95% CI: 0.54–1.49 mg N-$N_2O$/$m^2$/d) (Tables 1 and S3) is about 28% of the estimate for reservoirs in USA (3.67 mg N-$N_2O$/$m^2$/d) (Baron et al., 2013), but is 3.4-fold higher than the more recent estimated flux for global reservoirs (Table 2).

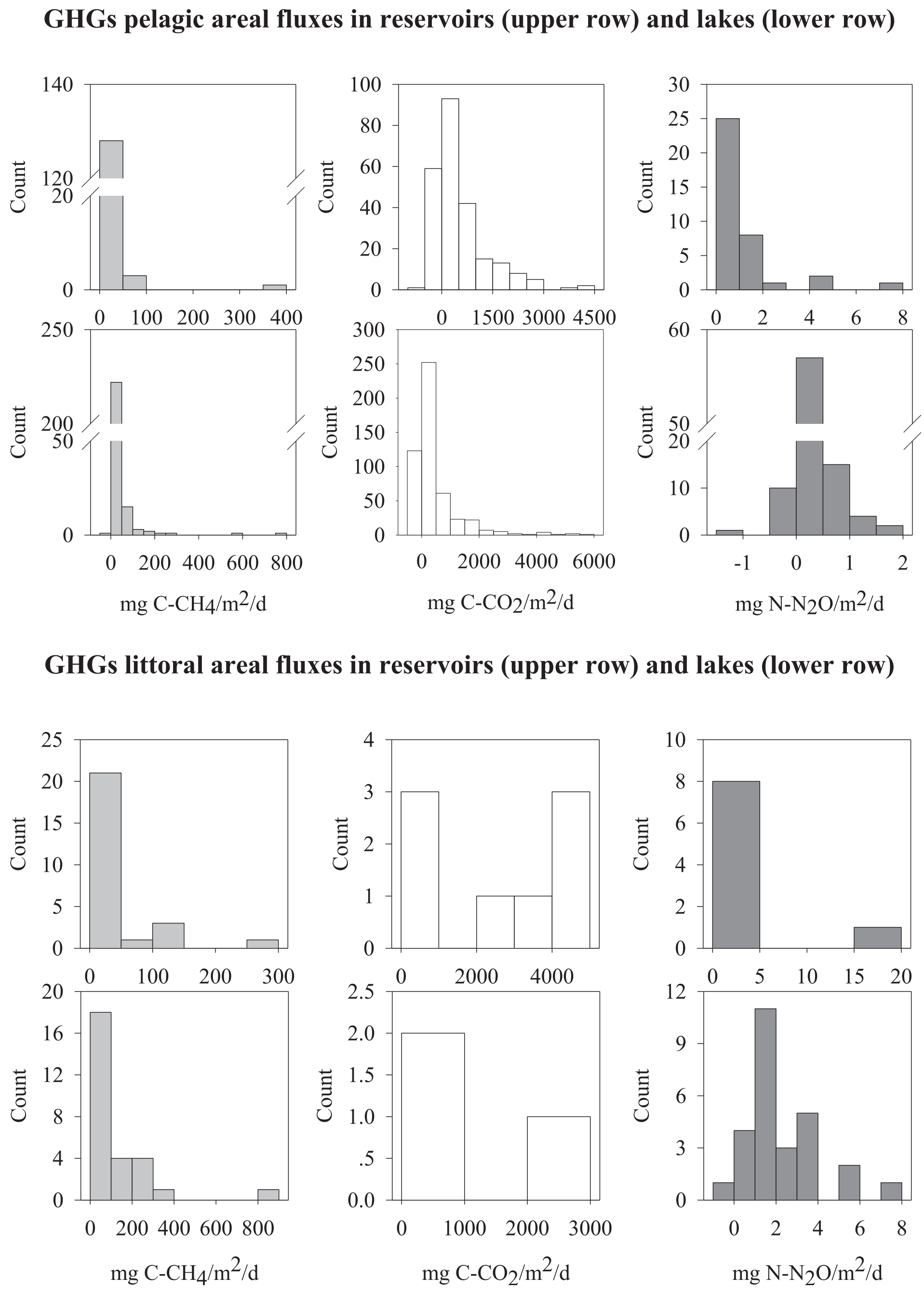


**Fig. 2.** Histograms showing GHGs areal fluxes *via* open waters and littoral zones for reservoirs and lakes, China.

All the reservoir drawdown areas were sources of GHGs to the atmosphere, with a range from 0.34 to 268.20 mg C-$CH_4$/$m^2$/d, 452.3–4348.2 mg C-$CO_2$/$m^2$/d, and 0.31–19.70 mg N-$N_2O$/$m^2$/d (Fig. 2; Supplementary Table S4). On average, drawdown areas showed 2.6–4.8-fold higher GHGs areal fluxes than reservoir pelagic waters in China (Table 1).

When upscaling emissions to the reservoir surface area, we estimated that reservoir pelagic areas emitted 0.08 (95% CI: 0.035–0.126) Tg C-$CH_4$ per year, 4.18 (3.40–4.96) Tg C-$CO_2$/y, and 7.97 (4.23–11.72) Gg N-$N_2O$/y (Tables 1 and 3). The reservoir pelagic emissions of $CH_4$ and $CO_2$ were comparable to the reservoir drawdown areas, while reservoir pelagic $N_2O$ emissions were around 1.5-fold higher than the drawdown emission (Table 1). Our newly estimated $CH_4$ emission was 1.7-fold higher than the previous $CH_4$ estimate from China's reservoirs (Table 2), which was likely due to our more complete coverage of data and inclusion of high emission rates particularly in drawdown areas. The majority (72%) of $CO_2$ equivalents from reservoirs occurred as $CO_2$, while $CH_4$ and $N_2O$ were responsible for 15% and 13% of radiative forcing, respectively, over a 100-year timespan.

### *3.2. Lake GHGs emissions in China*

Similar to reservoirs, all the lake systems were either $CH_4$ neutral or $CH_4$ sources. Most lakes (75.6%) were also sources of $CO_2$. Only 24.4% of open lake waters were net $CO_2$ sinks and 12.6% of

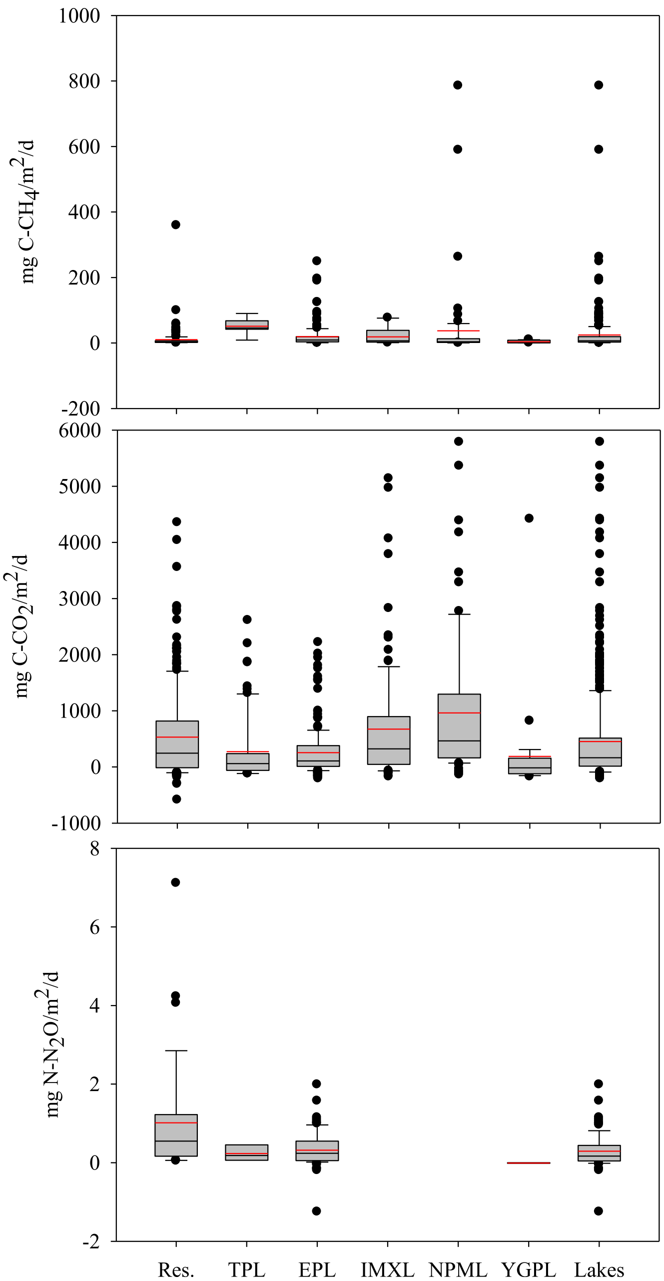


**Fig. 3.** Average reservoir and lake pelagic GHGs fluxes by box plots with whiskers (the black and red lines, lower and upper edges, bars and dots in or outside the boxes represent median and mean values, 25th and 75th, 5th and 95th, and <5th and >95th percentiles of all data, respectively). (For interpretation of the references to color in this figure legend, the reader is referred to the Web version of this article.)

lakes were net $N_2O$ sinks (Fig. 2). There are distinct differences in spatial variability and median fluxes of GHGs ($p < 0.05$ by Mann-Whitney Rank Sum Test; Fig. 3), with high average of $CH_4$ in TPL where lakes are mostly rich in DOC at the high altitude, and high average of $CO_2$ in NPML where lakes are mostly effected by carbon-rich wetlands at the high latitude. Overall, estimated areal GHGs fluxes of lake pelagic waters were $24.41 \pm 69.55$ (95% CI: 15.73–33.09) mg C-$CH_4$/m$^2$/d, $447.56 \pm 822.57$ (376–520) mg C-$CO_2$/m$^2$/d, and $0.29 \pm 0.42$ (0.21–0.38) mg N-$N_2O$/m$^2$/d (Fig. 3; Supplementary Table S3). Generally, lakes had lower fluxes of $CO_2$ and $N_2O$, but higher $CH_4$ fluxes, relative to reservoirs (Table 1).

Lake littoral zones had distinctly higher GHGs areal fluxes than the pelagic zones (Fig. 3; Supplementary Table S4). In average, littoral zones showed 5-fold higher mean $CH_4$ emission rate, 2.6-fold higher $CO_2$ and 7.4-fold higher $N_2O$ than open waters (Table 1). For the different geographic zones of lakes, the maximal ratio of GHGs emission rate in littoral zones to pelagic areas was 7.4 for $CO_2$ (IMXL), 10.9 for $CH_4$ (TPL) and 13.4 for $N_2O$ (TPL), respectively (Table 1). We also found distinct differences in emission rates of the three GHGs between lake littoral areas and reservoir drawdown zones ($p < 0.05$ by Mann-Whitney Rank Sum Test; Table S4), albeit comparable mean areal $N_2O$ fluxes were observed ($2.63 \pm 6.40$ vs $2.17 \pm 1.78$ mg N-$N_2O$/m$^2$/d for reservoir drawdown and lake littoral, respectively; Table 1). We estimated that lake pelagic areas emitted 0.96 (95% CI: 0.57–1.36) Tg C-$CH_4$/y, 10.2 (6.6–13.8) Tg C-$CO_2$/y, and 5.18 (0.02–10.34) Gg N-$N_2O$/y (Tables 1 and 3). The lake pelagic emissions of $CH_4$ and $CO_2$ were much higher than the lake littoral emissions, given that the pelagic area was 7.3 fold larger than the littoral area. Lake pelagic $N_2O$ emission, however, was around 72% of the littoral emission (Table 1).

Highest emissions of GHGs occurred in TPL, while YGPL had the lowest, ranging from $1.74 \pm 1.69$ to $676.91 \pm 310.86$ Gg C-$CH_4$/y, $77.9 \pm 297.6$ to $3601.9 \pm 7556.6$ Gg C-$CO_2$/y in the lake pelagic areas (Tables 1 and 3). Our new $CH_4$ emission estimate is reasonable considering the previous wide range (0.26–2.26 Tg C-$CH_4$/y) of emissions from very limited data (Table 2) (Yang et al., 2011a; Chen et al., 2013). The earlier higher estimate of China's lake methane emissions was based on several extremely high measurements (Yang et al., 2011a). In contrast to reservoirs, the majority of $CO_2$ equivalents from lakes occurred as $CH_4$ (50%) and $CO_2$ (45%), and $N_2O$ was responsible for 5% of radiative forcing, respectively, over a 100-year timeframe.

We combined lake littoral and pelagic areas into individual lake geographical zones to minimize the effects of the limited lake littoral data (Table 4). TPL and YGPL, respectively, showed the highest and lowest GHGs emissions. Emissions of $CH_4$ (2.08 Tg C-$CH_4$/y, 95% CI: 0.65–3.51) were 148% of the separated estimate of littoral and pelagic zones (Table 1), $CO_2$ (12.1 Tg C-$CO_2$/y, 95% CI: 7.8–16.4) was 76% and $N_2O$ (36.87 Gg N-$N_2O$/y, 95% CI: 18.44–55.30) was 298% (Table 4). GHGs emissions expressed as $CO_2$ equivalents (156.0 Tg $CO_2$eq/y, 95% CI: 66.9–245.2) were comparable to the separated estimates (Table 1).

### 3.3. Controls of GHGs areal fluxes of China's reservoirs and lakes

We collated lake and reservoirs characteristics that may explain GHGs fluxes. Similar to other climate zones such as arctic and boreal biomes, complex interactions of biological processes, trophic status, hydro-climatological factors, and organic matter are believed to drive GHGs emissions from China's reservoirs and lakes (Supplementary Table S5) (Bastviken et al., 2004; Rantakari and Kortelainen, 2005, 2008; Humborg et al., 2010; Halbedel and Koschorreck, 2013). Regression models for $N_2O$ were not attempted due to the small $N_2O$ dataset available.

The areal emissions of $CH_4$ from reservoirs had most significant correlations with air and surface water temperature when multiple biotic and abiotic variables were tested ($p < 0.05$; Table S5). This implies $CH_4$ production in anoxic sediments (usually the main methane source to lakes and reservoirs) is primarily controlled by temperature as observed elsewhere (Gudasz et al., 2010; Marotta et al., 2014; Wang et al., 2014). Also, many of China's reservoirs have gorge-type topography where deep water depth facilitates $CH_4$ oxidation (Bastviken et al., 2004; DelSontro et al., 2011; Xiao et al., 2013), as indicated separately by the significant negative associations between spatial heterogeneity in $CH_4$ areal fluxes and water depth in the two typical reservoirs (Yang et al., 2011b; Zheng et al., 2011).

**Table 1**
GHGs estimates (average ± S.D.) from reservoirs and lakes in China (abbreviations of lake regions please refer to Fig. 1).

| | Area flux (milligrams per square meter per day) | | | Annual emission (G C or N per year) | | | Annual $CO_2$ equivalents (Tg $CO_2$ Eq per year) | | | | Area |
|---|---|---|---|---|---|---|---|---|---|---|---|
| | C-$CH_4$ | C-$CO_2$ | N-$N_2O$ | C-$CH_4$ | C-$CO_2$ | N-$N_2O$ | $CH_4$ | $CO_2$ | $N_2O$ | Total | $km^2$ |
| **Reservoir** | | | | **150.97** | **9167.0** | **13.14** | **6.85** | **33.61** | **6.15** | **46.61** | **26870** |
| Pelagic areas | 10.254 ± 33.374 | 532.485 ± 781.744 | 1.016 ± 1.433 | 80.45 ± 261.85 | 4177.9 ± 6133.6 | 7.97 ± 11.24 | 3.65 | 15.32 | 3.73 | 22.70 | 21496 |
| Drawdown | 35.954 ± 60.522 | 2543.50 ± 1660.53 | 2.633 ± 6.403 | 70.52 ± 118.71 | 4989.1 ± 3257.2 | 5.17 ± 12.56 | 3.20 | 18.29 | 2.42 | 23.91 | 5374 |
| **Lakes** | | | | | | | | | | | |
| **Pelagic areas** | **24.406 ± 69.546** | **447.56 ± 822.57** | **0.293 ± 0.417** | **964.66** | **10209.4** | **5.18** | **43.72** | **37.42** | **2.43** | **83.57** | **72364.16** |
| TPL | 51.256 ± 25.538 | 272.74 ± 572.19 | 0.233 ± 0.215 | 676.91 ± 310.86 | 3601.9 ± 7556.6 | 3.08 ± 2.84 | 30.69 | 13.21 | 1.44 | 45.33 | 36182.08 |
| EPL | 19.422 ± 35.010 | 256.35 ± 417.65 | 0.319 ± 0.271 | 128.25 ± 231.18 | 1692.7 ± 2757.9 | 2.11 ± 2.85 | 5.81 | 6.21 | 0.99 | 13.01 | 18091.04 |
| IMXL | 18.639 ± 25.139 | 674.79 ± 987.18 | | 73.85 ± 99.60 | 2673.5 ± 3911.1 | | 3.35 | 9.80 | | 13.15 | 10854.62 |
| NPML | 37.377 ± 124.727 | 963.62 ± 1260.61 | | 83.91 ± 280.02 | 2163.4 ± 2830.2 | | 3.80 | 7.93 | | 11.74 | 6150.954 |
| YGPL | 4.371 ± 4.256 | 196.82 ± 751.93 | −0.008 ± 0.008 | 1.74 ± 1.69 | 77.9 ± 297.6 | −0.003 ± 0.003 | 0.08 | 0.28 | −0.001 | 0.34 | 1085.462 |
| **Littoral zones** | **121.491 ± 164.021** | **1175.41 ± 1553.22** | **2.168 ± 1.776** | **446.56** | **5771.84** | **7.21** | **20.25** | **21.16** | **3.38** | **44.79** | **9867.84** |
| TPL | 144.610 ± 218.206 | 2967 | 3.119 ± 1.310 | 260.43 ± 392.96 | 5343.1 | 5.62 ± 2.36 | 11.81 | 19.59 | 2.63 | 34.03 | 4933.92 |
| EPL | 78.184 ± 77.830 | 351.49 | 1.768 ± 1.821 | 70.40 ± 70.08 | 316.5 | 1.59 ± 1.64 | 3.19 | 1.16 | 0.75 | 5.1 | 2466.96 |
| IMXL | 138.84 ± 129.859 | 207.75 | | 75.01 ± 70.16 | 112.24 | | 3.4 | 0.41 | | 3.81 | 1480.176 |
| NPML | 131.22 | | | 40.17 | | | 1.82 | | | 1.82 | 838.7664 |
| YGPL | 10.26 | | | 0.55 | | | 0.03 | | | 0.03 | 148.0176 |

$CO_2$equiv. in 100-year time span ($GWP_{100}$) was calculated as the data for $CO_2$ plus the $CH_4$ data multiplied by 34 and $N_2O$ multiplied by 298 on the basis of the global potential of $CH_4$ and $N_2O$.
$GWP_{100}$ denotes global warming potential for the 100 year metrics.
Negative sign represents net GHGs sink.

**Table 2**
Diffusive GHGs emissions from China's reservoirs and lakes compared with other freshwater ecosystems and anthropogenic activities.

| | Surface area | Areal flux | | | GHG emission | | | Source |
|---|---|---|---|---|---|---|---|---|
| | | C-$CH_4$ | C-$CO_2$ | N-$N_2O$ | C-$CH_4$ | C-$CO_2$ | N-$N_2O$ | |
| | $10^5$ $km^2$ | $mg/m^2/d$ | $mg/m^2/d$ | $mg/m^2/d$ | Tg/y | Tg/y | Gg/y | |
| China's reservoirs | 0.2687 | 10.25 ± 33.37 | 532.49 ± 781.74 | 1.016 ± 1.433 | 0.151 | 9.17 | 13.14 | This study |
| China's lakes | 0.82232 | 24.41 ± 69.55 | 447.56 ± 822.57 | 0.293 ± 0.417 | 1.411 | 15.98 | 12.39 | This study |
| Reservoirs & lakes in China | | | | | 1.56 | 25.15 | 25.53 | This study |
| China's total emission | | | | | 40 | 1600 | 2150 | |
| China's reservoirs | | | | | 0.086 | | | Chen et al., 2013 |
| China's lakes | | | | | 0.257 | | | Chen et al., 2013 |
| China's lakes | | | | | 2.25 | | | Yang et al., 2011a |
| Temperate reservoirs[$] | 9 | 15 | 381.82 | | 3 | 81.82 | | St Louis et al., 2000 |
| Temperate reservoirs | 1.2 | 11.64[a] | | | 0.53[a] | | | Bastviken et al., 2011 |
| Temperate reservoirs | 1.3 | 14.79 | 313.82 | | 0.7 | 15 | | Hertwich, 2013 |
| Temperate lakes | 13.3 | 7.42 | | | 3.6 | | | Bastviken et al., 2011 |
| Temperate lakes and reservoirs | 14.47 | 7.76 | 219.18 | | 4.1 | 80 | | Aufdenkampe et al., 2011; Bastviken et al., 2011 |
| Global reservoirs[b] | 15 | 95.89 | 498.14 | | 52.5 | 273 | | St Louis et al., 2000 |
| Global reservoirs | | | | | | 280 | | Cole et al., 2007 |
| Global reservoirs | 5 | 82.2[a] | | | 15[a] | | | Bastviken et al., 2011 |
| Global reservoirs | 3.1 | 120[a] | 330 | 0.30 | 13.3[a] | 36.8 | 30 | Deemer et al., 2016 |
| Global lakes | | | | | 6–36 | | | Bastviken et al., 2004 |
| Global lakes | | | | | | 110 | | Cole et al., 2007 |
| Global lakes | | | 345.73 | | | 530 | | Tranvik et al. 2009 |
| Global lakes | 37.4 | 5.3 | | | 7.3 | | | Bastviken et al., 2011 |
| Lakes and reservoirs | 30 | | 292.24 | | | 320 | | Raymond et al. 2013 |
| Lakes and reservoirs | 28–45.4 | | 479.08 | | | 640 | | Aufdenkampe et al., 2011 |
| Global inland waters | 46 | | | | 69.8[a] | | | Bastviken et al., 2011 |
| Global inland waters | 36.2 | | | | | 2120 | | Raymond et al. 2013 |
| Anthropogenic sources | | | | | 400 | 10000 | 6900 | Myhre et al., 2013 |

Areas between latitude $25^0$-$54^0$, can be simply considered as temperate zone for large scale studies (Bastviken et al., 2011). In order to compare our studies to other regional/large scale results, we do not extract subtropical lakes or reservoirs from temperate biome in our study.
[a] Including ebullition and diffusion driven flux.
[b] -Downscaling approach of surface area was used for GHGs emissions for comparison with our estimates.

The areal fluxes of $CO_2$ from reservoirs were positively correlated to air temperature, total nitrogen (TN) and total phosphorous (TP), but negatively correlated with chlorophyll-a (Chl-a), dissolved oxygen (DO) and pH (Supplementary Table S5). Prior studies also reported strong positive correlations between nutrients and $CO_2$ emissions (Rantakari and Kortelainen, 2008; Teodoru et al., 2009). The negative correlation between $CO_2$ emission and DO concentration could indicate *in-situ* respiration of organic C as an important source of the $CO_2$ supersaturation that drives emissions. However, this negative correlation is concurrently controlled by photosynthesis producing DO and consuming $CO_2$, thus lowering $CO_2$ supersaturation and $CO_2$ emissions, as well as increasing pH.

We further identified new predictors of GHGs areal fluxes using a multiple-regression model. The most robust multiple-regression

**Table 3**
Uncertainty estimates (95% confidence intervals) of annual fluxes and annual $CO_2$ equivalents of GHGs in lakes and reservoirs in China (abbreviations of lake regions please refer to Fig. 1).

| | | Annual flux (Gg/y) | | Annual $CO_2$ Equivalents (Tg $CO_2$ eq/y) | |
|---|---|---|---|---|---|
| | | 95% Confidence Interval | | 95% Confidence Interval | |
| **Reservoir** | | Lower bound | Upper bound | Lower bound | Upper bound |
| *Pelagic* | | | | | |
| C-$CH_4$ | | 35.37 | 125.54 | 1.60 | 5.69 |
| C-$CO_2$ | | 3396.31 | 4959.49 | 12.45 | 18.18 |
| N-$N_2O$ | | 4.23 | 11.72 | 1.98 | 5.49 |
| *Pelagic + Drawdown* | | | | | |
| C-$CH_4$ | | 105.89 | 196.06 | 4.80 | 8.89 |
| C-$CO_2$ | | 8385.41 | 9948.59 | 30.74 | 36.47 |
| N-$N_2O$ | | 9.40 | 16.89 | 4.40 | 7.91 |
| **Lakes** | | | | | |
| *Pelagic areas* | | | | | |
| TPL | C-$CH_4$ | 437.96 | 915.86 | 19.85 | 41.52 |
| | C-$CO_2$ | 1909.35 | 5294.53 | 7.00 | 19.41 |
| | N-$N_2O$ | −1.44 | 7.59 | −0.68 | 3.56 |
| EPL | C-$CH_4$ | 90.43 | 166.06 | 4.10 | 7.53 |
| | C-$CO_2$ | 1312.94 | 2072.49 | 4.81 | 7.60 |
| | N-$N_2O$ | 1.47 | 2.75 | 0.69 | 1.29 |
| IMXL | C-$CH_4$ | 24.32 | 123.38 | 1.10 | 5.59 |
| | C-$CO_2$ | 1920.22 | 3426.7 | 7.04 | 12.56 |
| NPML | C-$CH_4$ | 13.97 | 153.86 | 0.63 | 6.98 |
| | C-$CO_2$ | 1512.26 | 2814.61 | 5.54 | 10.32 |
| YGPL | C-$CH_4$ | 0.66 | 2.80 | 0.03 | 0.13 |
| | C-$CO_2$ | −18.60 | 174.55 | −0.07 | 0.64 |
| | N-$N_2O$ | −0.006 | 0 | −0.003 | 0 |
| *Lakes pelagic total* | | | | | |
| C-$CH_4$ | | 567.3 | 1362.0 | 25.71 | 61.75 |
| C-$CO_2$ | | 6636.2 | 13782.9 | 24.32 | 50.53 |
| N-$N_2O$ | | 0.02 | 10.34 | 0.01 | 4.84 |
| *Lakes pelagic + littoral* | | | | | |
| C-$CH_4$ | | 1013.61 | 1808.26 | 45.95 | 81.97 |
| C-$CO_2$ | | 12375.35 | 19581.65 | 45.37 | 71.8 |
| N-$N_2O$ | | 7.23 | 17.55 | 3.39 | 8.22 |
| **Reservoirs + Lakes total** | | | | 134.65 | 215.26 |

**Table 4**
Lake GHGs areal fluxes and emissions without separation of littoral area from lakes (we consider lake geographical zones, while we combine lake pelagic and littoral areas in individual lake zone).

| | Size | Areal flux (mg C or N/m$^2$/d) | | | Annual emission (Gg C or N/y) | | |
|---|---|---|---|---|---|---|---|
| | | Mean ± S.D. | 95% CI | | Mean | 95% CI | |
| | | | Lower Bound | Upper Bound | | Lower Bound | Upper Bound |
| **Total lakes** | | | | | | | |
| C-$CH_4$ | 277 | 34.50 ± 88.97 | 23.92 | 45.08 | 2083.41 | 652.42 | 3514.41 |
| C-$CO_2$ | 506 | 456.57 ± 883.28 | 383.13 | 530.01 | 12090.96 | 7814.17 | 16367.75 |
| N-$N_2O$ | 116 | 0.73 ± 1.22 | 0.51 | 0.95 | 36.87 | 18.44 | 55.30 |
| **TPL** | | | | | | | |
| C-$CH_4$ | 22 | 106.42 ± 172.12 | 30.11 | 182.73 | 1597.08 ± 2583.10 | 451.80 | 2742.36 |
| C-$CO_2$ | 80 | 306.42 ± 643.42 | 163.23 | 449.61 | 4598.53 ± 9656.10 | 2449.67 | 6747.39 |
| N-$N_2O$ | 12 | 2.16 ± 1.77 | 1.03 | 3.28 | 32.37 ± 26.52 | 15.52 | 49.22 |
| **EPL** | | | | | | | |
| C-$CH_4$ | 153 | 22.11 ± 39.50 | 15.8 | 28.42 | 165.91 ± 296.38 | 118.57 | 213.25 |
| C-$CO_2$ | 206 | 256.81 ± 416.68 | 199.57 | 314.05 | 1927.00 ± 3126.66 | 1497.5 | 2356.51 |
| N-$N_2O$ | 98 | 0.60 ± 1.05 | 0.39 | 0.81 | 4.50 ± 7.86 | 2.93 | 6.08 |
| **IMXL** | | | | | | | |
| C-$CH_4$ | 24 | 48.69 ± 83.43 | 13.46 | 83.92 | 219.21 ± 375.60 | 60.61 | 377.81 |
| C-$CO_2$ | 107 | 670.42 ± 983.55 | 481.91 | 858.93 | 3018.37 ± 4428.13 | 2169.65 | 3867.09 |
| **NPML** | | | | | | | |
| C-$CH_4$ | 65 | 38.82 ± 124.30 | 8.02 | 69.62 | 99.04 ± 317.11 | 20.47 | 177.62 |
| C-$CO_2$ | 75 | 963.62 ± 1269.62 | 673.58 | 1253.67 | 2458.44 ± 3216.15 | 1718.48 | 3198.41 |
| **YGPL** | | | | | | | |
| C-$CH_4$ | 13 | 4.82 ± 4.39 | 2.17 | 7.48 | 2.17 ± 1.98 | 0.98 | 3.37 |
| C-$CO_2$ | 39 | 196.82 ± 751.93 | −46.93 | 440.57 | 88.61 ± 338.54 | −21.13 | 198.35 |
| N-$N_2O$ | 6 | −0.008 ± 0.008 | −0.016 | 0 | −0.004 ± 0.004 | −0.007 | 0 |

model for the reservoir $CO_2$ emission rate included TP and Chla as independent variables and explained 40% of the variation in $CO_2$ fluxes. The model for areal $CH_4$ fluxes included TP, DO and air temperature, and explained 36% of variations in $CH_4$ flux (Supplementary Table S6). Like the GHGs emission rates of reservoirs that were predicted using nutrients and productivity, lake $CH_4$

areal flux was predicted by TP, DOC and Chl-a, and $CO_2$ areal flux by TP (49% and 33% of variances are explained, respectively; Supplementary Table S6).

*3.4. Upscaling GHGs emissions from China's reservoirs and lakes*

Clearly, reservoirs and lakes in China are important GHG sources. Lakes have 9.3-fold greater $CH_4$ fluxes, and 1.7-fold greater $CO_2$ fluxes than reservoirs, whereas, lakes and reservoirs have comparable $N_2O$ fluxes. Combined, the total estimated emissions of $CH_4$ (1.56 Tg C-$CH_4$/y; 95% CI: 1.12–2.00), $CO_2$ (25.2 Tg C-$CO_2$/y; 95% CI: 20.8–29.5) and $N_2O$ (25.5 Gg N-$N_2O$/y; 95% CI: 16.6–34.4) from reservoirs and lakes account for 3.9%, 1.6% and 1.2% of anthropogenic $CH_4$, $CO_2$ and $N_2O$ emissions in China (Tables 2 and 3).

Our data implies emissions of 202.6 (95% CI: 106.8–298.5) Tg $CO_2$ equivalent per year (if littoral zone and pelagic zone are combined) (Tables 1 and 4), and 175.0 (95% CI: 134.7–215.3) Tg $CO_2$ equivalent per year (if the two zones are separated) (Table 3) in 100-year horizon for lakes and reservoirs (73.4% of total radiative forcing contributed by lakes), translating into the global-warming potential of $CH_4$, $CO_2$ and $N_2O$ (Tables 1 and 3). This is equal to about 14.1%–22.6% of the estimated terrestrial carbon sink of China ($260 \pm 90$ Tg C-$CO_2$/y) (Piao et al., 2009; Tian et al., 2011). This indicates that large amounts of the estimated land $CO_2$ sink is returned to the atmosphere through reservoirs and lakes. Therefore, our results indicate that China's lakes and reservoirs are a disproportionately high contributor of GHGs given their minor contribution (ca. 1.1%) to the China's land surface.

## 4. Discussion

*4.1. Implications of Chinese inland water GHG emission on global budgets*

Our new estimates of China's reservoir diffusive GHGs emissions contributed significantly to GHGs budgets in the temperate zone. Diffusion-driven annual $CH_4$ emission from China's reservoirs represented 21.6%–34.8% of the total emissions from temperate reservoirs, comparable to the area proportion (21%) of China's reservoirs to the temperate biome (Table 2). The total annual emission of $CO_2$ from China's reservoirs made up 61%–78% of the temperate reservoir $CO_2$ flux, more than 3-fold higher than its proportion of surface area (St Louis et al., 2000; Hertwich, 2013) (Table 2). Annual $N_2O$ emissions comprised 35.5% of the reservoir $N_2O$ emission in the USA, much lower than the ratio of reservoir surface area in China (26870 $km^2$) to USA (27600 $km^2$) (Baron et al., 2013). If we incorporated the more recent reservoir data in the temperate biome (Deemer et al., 2016), there were no significant differences in $CO_2$ and $CH_4$ diffusive areal fluxes between China's reservoirs and temperate reservoirs including China or excluding China ($p > 0.05$ by Mann-Whitney Rank Sum Test), while reservoir $N_2O$ emission rate was significantly higher in China than in the temperate biome (Fig. 4). In total, GHGs emissions from China's lakes and reservoirs, expressed $CO_2$ equivalents, accounted for 2.5–3.8% of global lakes and reservoirs combined (1.25–2.30 Pg C-$CO_2$eq/y), comparable to the surface area proportion (2.0–3.4%) of lakes and reservoirs in China to globe (DelSontro et al., 2018).

We found that reservoir pelagic areal fluxes of $CO_2$, and $N_2O$ in China were higher than or at least proximate to global estimates (Table 2). The lower pelagic areal $CH_4$ emissions (one tenth of the global averages) (Table 2) can be explained by the omission of ebullitive fluxes, i.e., ebullition may exceed diffusion by 2.4–3.4-fold (DelSontro et al., 2018), and a preponderance of high $CH_4$ flux estimates in tropical reservoirs or other temperate areas outside of China (St Louis et al., 2000; Deemer et al., 2016). Our findings are consistent with the common view that low latitude reservoirs have higher $CH_4$ emission rates than the reservoirs in the temperate biome, albeit high emission rates were reported in the mid-latitude reservoirs in North America, Europe and Australia (Deemer et al., 2016).

Mean areal fluxes of GHGs would be 1.3–4.2-fold higher in temperate reservoirs including China ($9.23 \pm 28.39$ mg C-$CH_4$/$m^2$/d, $440.89 \pm 664.76$ mg C-$CO_2$/$m^2$/d, $0.60 \pm 0.14$ N-$N_2O$/$m^2$/d) than temperate reservoirs excluding China ($7.18 \pm 13.87$ mg C-$CH_4$/$m^2$/d, $293.96 \pm 370.79$ mg C-$CO_2$/$m^2$/d, $0.14 \pm 0.31$ N-$N_2O$/$m^2$/d) (Fig. 4). Consequently, GHG emissions from temperate reservoirs could be revised to be $0.40 \pm 1.24$ (95% CI: 0.23–0.58) Tg C-$CH_4$/y as diffusion, $19.31 \pm 29.12$ (95% CI: 16.40–22.22) Tg C-$CO_2$/y, and $26.2 \pm 49.8$ (95% CI: 14.4–38.0) Gg N-$N_2O$/y. Therefore, our comprehensive analysis of GHGs emissions from Chinee reservoirs demonstrated that previous estimates based largely on European and North American systems likely underestimated inland water's contribution to global GHGs budgets, and highlights the need of including more data from China and other under sampled areas in developing countries in global upscaling exercises.

For lakes, our estimated $CH_4$ flux accounted for 39% of the total $CH_4$ emissions from the temperate zone, which was 6.3-fold higher than China's lakes proportion of surface area (Table 2). The total emission of $CO_2$ from lakes in China was 24.6% of the temperate fluxes, 4-fold higher than the contribution of surface area (Table 2) (Aufdenkampe et al., 2011). However, $N_2O$ emission from China's lakes was only 28.8% the emission from USA lakes (Baron et al., 2013). This offers further support to our suggestion that China's reservoirs and lakes were a disproportionate contributor to temperate inland water emissions of $CH_4$ and $CO_2$, but not $N_2O$.

We reported GHGs emissions from natural lakes and reservoirs in China and build on prior studies elaborating on the combined effects of GHGs emissions from natural lakes and artificial reservoirs (Bastviken et al., 2011; Raymond et al., 2013; Deemer et al., 2016). While emissions from reservoirs (anthropogenic systems) can be related to a new source to the atmosphere, emissions from lakes will usually represent a natural GHG pathway unless the lakes and their catchment have been modified.

Anthropogenic GHGs emissions from reservoirs need to consider the pre-impoundment fluxes. Reservoir $CO_2$ emission declines quickly in the years following impoundment (Barros et al., 2011; Prairie et al., 2017). Life-cycle analysis demonstrated that 25% of the cumulative $CO_2$ flux was attributable to creation of reservoirs (Prairie et al., 2017). This is of great importance due to China's rapid growth in reservoir construction. Carbon sedimentation is a potential offset to reservoir C emissions especially in China, where 0.6 Gt/y particulate materials can be trapped by dams (Chu et al., 2009). Assuming a minimum POC content of 0.5% in suspended sediment trapped by dams (Lu et al., 2012) indicates that around 3 Tg C/y could be discounted from the estimated reservoir $CO_2$ emissions to the atmosphere. The resulting net $CO_2$ emission would be 6.2 Tg C-$CO_2$/y, which is 33% lower than the total estimated emissions from reservoirs. This analysis highlights the need for developing full carbon budgets for new reservoirs to quantify their net GHG footprint (Prairie et al., 2017).

*4.2. National and regional conditions affecting GHG production and emission*

In comparison to global lakes, China's lakes have higher loadings of nutrients and are usually more eutrophic (Supplementary Table S2) (Bastviken et al., 2011; Yang et al., 2011a). High photosynthetic rates and high organic loads increase the substrate for methanogenesis and consequently contribute to the high diffusion-driven emission rate, i.e., the 3.3-fold higher $CH_4$ in lake pelagic

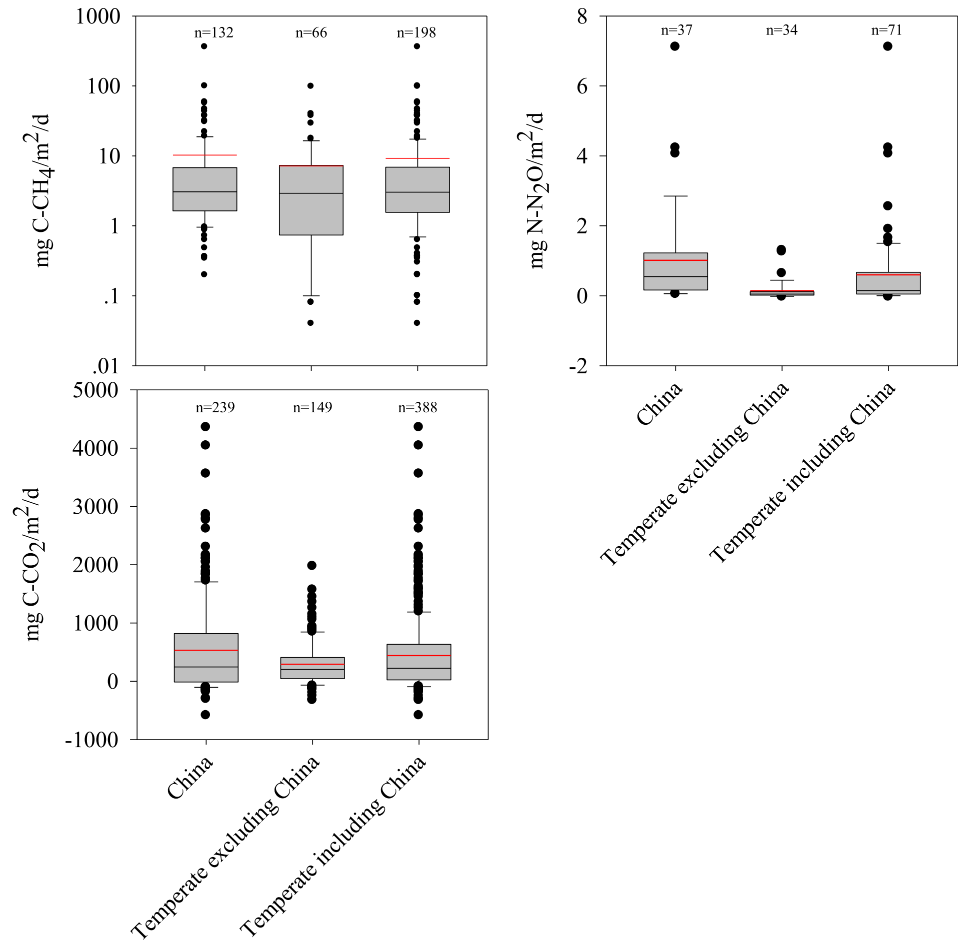


**Fig. 4.** Reservoir pelagic GHGs areal fluxes in China and other temperate reservoirs (Diffusive areal fluxes from other temperate reservoir data are taken from Deemer et al. (2016). (There is no significant difference in reservoir diffusive $CH_4$ areal fluxes and $CO_2$ areal fluxes among China, temperate excluding China and temperate including China; Reservoir $N_2O$ areal fluxes in China is significantly higher than the temperate reservoirs with or without China's reservoirs) (Symbols are similar to Fig. 3).

areas of China than in temperate lakes in North America and Europe (7.42 mg C-$CH_4$/$m^2$/d)[2]. The $CH_4$ emission rate is also much higher (4.6 times) than diffusive emission rate of global lakes (Table 2).

Our key findings are indicative of highest areal emission rates of $CH_4$, $N_2O$ and $CO_2$ from littoral or drawdown zones of lakes and reservoirs (Table 1). Elevated levels of sedimentary organic matter, combined with periodically inundated plant biomass, are closely linked to distinctly higher emission rates of $CH_4$ and $CO_2$ in the littoral (or drawdown) zones of both lakes and reservoirs (Fearnside and Pueyo, 2012; Hertwich, 2013). Moreover, diffusive $CH_4$ and $CO_2$ areal fluxes were significantly different between different lake geographic zones with the highest emission rates of $CH_4$ in TPL, and $CO_2$ in IMXL and NPML ($p < 0.05$ by Mann-Whitney Rank Sum Test; Fig. 3). These three geographic lake zones particularly the TPL have extremely higher DOC concentrations (Supplementary Fig. S9). DOC concentrations are weakly correlated with primary production (Chl-a) in lakes ($r = -0.29$, $p < 0.01$ by Spearman's rho), implying that DOC is likely allochthonous (i.e., surrounding soils, groundwater or upper catchment) rather than autochthonous. The low DOC, as well as high nutrients and primary production, resulted in the low $CH_4$ and $CO_2$ emissions in EPL and YGL lake zones (Table 1; Fig. 3) as observed elsewhere (Cole et al., 2007; Tranvik et al., 2009; Knoll et al., 2013).

Monsoon climate in East, Centre, Southwest and South China, where reservoirs concentrate, and changing land use largely increases reservoir carbon loads and turbidity, which limits light penetration and fuels heterotrophic activity and drives $CO_2$ production. The concentrated rainfall even with high temperature decreases reservoir $CO_2$ flux in the monsoonal season (Li and Zhang, 2014b). The monsoonal particulate carbon may be highly recalcitrant, limiting respiration and masking the coupling between allochthonous organic carbon and $CO_2$ production (Supplementary Table S5) (Mayorga et al., 2005). Detailed seasonal observations, including rainfall events and monsoon cycles, are unavailable but essential to refine our estimates.

The averages of GHGs fluxes were not clearly linked to reservoir ages (data from Supplementary Table S1), which is different than a global analysis (Barros et al., 2011). The common practice of biomass clearing before impoundment in China can reduce the flooded biomass and prevent the formation of GHGs. In addition, the initial intense degradation of labile biomass and soil organic carbon in tropical reservoirs results in negative correlations between GHGs emissions and age (Barros et al., 2011; Fearnside and Pueyo, 2012). Congruent with global analyses excluding tropical reservoirs, there were no significant correlations between GHGs fluxes and latitude for China's temperate reservoirs (Barros et al., 2011).

Our findings highlighted the importance of phosphorus, aquatic productivity and organic carbon for water-air interface GHGs emissions, which were in agreement with the recent studies either using global reservoir data (Deemer et al., 2016) or diffusive $CH_4$ data from lakes in North American and Eurasia (Bastviken et al., 2004), as well as the combined data from global reservoirs and lakes (DelSontro et al., 2018). Our models for GHGs areal emissions from reservoirs and lakes can explain 33%–49% of the variations (Supplementary Table S6), which are comparable or better than other models (Bastviken et al., 2004; Deemer et al., 2016; DelSontro et al., 2018). Such models can help us to define the most important drivers of GHG areal fluxes in reservoirs and lakes of China.

### 4.3. Limitations of this study

Similar to other studies at national and global scales, our new estimates of GHGs emissions from China's reservoirs and lakes are also impacted by data limitations and uncertainties. Firstly, limited measurements are assumed to represent national observations, and often these measurements do not include $CH_4$ bubbles. This certainly contributes to large uncertainty of GHGs emissions because their areal fluxes are spatially and temporally heterogeneous (Supplementary Tables S1 and S2). Furthermore, not including ebullition biases our estimates low For example, field measurements in a lake (Huahua) of TPL indicated that bubbling $CH_4$ areal flux was 9-fold higher than its diffusive areal flux (Zhu et al., 2016). This is three times the ratio of $CH_4$ ebullition to $CH_4$ diffusion-driven flux from temperate lakes (Bastviken et al., 2011). If this is the case everywhere, an additional 2.8–11.3 Tg C-$CH_4$/y would be emitted from Chinese lakes due to $CH_4$ bubbling (the upper and lower levels are based on the ratio of bubbling flux to diffusive flux in TPL and temperate lakes). Moreover, the available dataset does not allow for an assessment of pulses of emissions when hypolimnic water usually enriched in GHGs emerges at the surface.

Other alterative flux pathways including rivers downstream of dams and dam spillways and turbines were not included in the GHGs emission estimates. Prior studies reported that river stretches directly downstream of dams constitute a significant fraction (9–33% for $CH_4$ and 2–32% for $CO_2$) of the emissions across the reservoir surfaces (Guerin et al., 2006; Kemenes et al., 2007, 2011; Teodoru et al., 2015). Degassing occurs when the hypolimnic waters rich in dissolved gases pass through turbines and spillways due to rapid depressurization and aeration. Past studies on tropical reservoirs showed that $CH_4$ emissions from turbines and spillways accounted for a magnitude of nine times the emission from reservoir surface (Roehm and Tremblay, 2006; Fearnside and Pueyo, 2012). Valley-type Chinese reservoirs have relatively small surface area with large water discharge and turbine depth greater than 30 m, clearly resulting in a larger proportion of GHGs emissions from turbines and spillways. Albeit uncertainties are still large, our new dataset advances our understanding of inland waters' GHGs emissions.

### 4.4. Policy implications and recommendations

Phosphorus (P) and Chla were the best predictors of reservoir and lake GHGs areal fluxes. This deserves particular attention because phytoplankton growth and bacterioplankton production are more often phosphorus-limited in lakes and reservoirs in China as reflected by high N:P ratios (Tables S1 and S2), similar to other lakes elsewhere (Chrzanowski and Grover, 2001; Vrede, 2005; Krist et al., 2016). Our findings suggest that P-loading reduction would be beneficial to mitigate $CH_4$ and $CO_2$ emissions. Specifically, the carbon-rich TPL region (Tibetan Plateau) has $CH_4$ emissions that are responsible for 68% of the radiative forcing from pelagic areas (Table 1). Since the Tibetan Plateau is highly vulnerable to climate change, increasing temperatures in this region could result in additional GHGs emissions. Thus, our work provides a crucial step in identifying potential management priorities for the reduction of GHGs emissions from natural and artificial lakes. Phosphate control should be prioritized in TPL and NPML with higher GHGs areal fluxes.

A total of 98,000 reservoirs have caused highly-regulated river flows in China, particularly in the Yangtze River basin with 50,000 reservoirs (MWR, 2016). Increasing anthropogenic nutrient inputs have driven lakes and reservoirs into a more autotrophic state, thus reducing the average $pCO_2$ in the river network (Wang et al., 2007). Eutrophication, however, increases $CH_4$ areal fluxes from the lentic systems (Deemer et al., 2016). These man-made reservoirs are now acknowledged as non-carbon neutral (Deemer et al., 2016), and GHGs emissions could discount the "green" credentials of hydropower (Fearnside, 2005). In order to test the green credentials of China's hydropower network, we compared GHGs emissions from reservoirs to fossil alternatives. GHGs emissions released by hydropower reservoirs are only 5%–9% of the thermo-power emissions over a 100-year timespan (Table 5) (dos Santos et al., 2006), but the hydropower generation accounts for 18.9% of the total energy (5811 TWh) produced in China. The analysis further indicates that hydroelectric reservoirs can reduce carbon emission by 500–953 Tg $CO_2$ eq per year in comparison to equivalent coal-fired plant alternatives (Table 5).

GHGs emissions from inland waters such as reservoirs and lakes are now gaining increased attention. However, inland water data remain scarce and fragmented with very little spatial and temporal resolution. Our work reveals that China's reservoirs and lakes may disproportionally contribute to temperate GHGs emissions. Our new estimated emissions of GHGs from China's lakes and reservoirs account for 14–23% of China's terrestrial carbon sink, even though these aquatic systems contribute to only 1.1% of China's mainland area. With the current boom in regional and global dam constructions (Zarfl et al., 2015), GHGs emissions from reservoirs including reservoir water surfaces, turbines and spillways and river downstream dam will represent large fraction of anthropogenic $CO_2$ equivalents. The rapid expansion of China's reservoir area for hydropower generation will result in increases in GHGs emissions. Further research is needed to evaluate impacts of the expansion in reservoir area on GHGs emissions, as well as extending existing datasets to cover spatial and temporal dynamics.

## 5. Conclusion

The study provides new insights into magnitude and controls on diffusion-driven emissions of GHGs $CH_4$, $CO_2$ and $N_2O$ from China's lakes and reservoirs. Our estimates of national scale GHG budgets are the only estimates based on unbiased, large-scale regional sampling that are extrapolated to the whole China, resolving the magnitude of GHG emissions from inland waters as well as the first

**Table 5**
Comparison of emissions from hydropower reservoirs with equivalent thermo-power plants.

| | Emission | Total emission |
|---|---|---|
| | g $CO_2$eq/kWh | Tg $CO_2$eq/y |
| Hydropower[a] | 46.6 | 46.6 |
| Coal (modern plant) | 1000 | 1000 |
| IGCC (coal)[b] | 798 | 798 |
| Diesel | 717 | 717 |
| Natural gas | 545 | 545 |

The comparable analyses are reasonable due to that more than 80% of reservoir water surfaces are contributed by hydropower reservoirs based on China's reservoirs registered in ICOLD (International Commission on Large dams).
[c]C emission per kWh by fossil is from dos Santos et al. (2006).
[a] 1000 billion kWh per year for hydropower generation of China.
[b] Integrated Gasification Combined Cycle (IGCC).

Chinese estimates of $N_2O$ emissions. China's lake and reservoirs seem to emit 1.56 Tg C-$CH_4$/y and 25.2 Tg C-$CO_2$/y. Expressed as $CO_2$ equivalents, these correspond to 175.0 (134.7–215.3) Tg $CO_2$ equivalent, with 73.4% of this forcing contributed by lakes. These aquatic sources are 14.1%–22.6% of China's estimated terrestrial carbon sink, implying a disproportionally high contribution to national GHGs emissions. Our investigation also identifies characteristics of lakes and geographic areas that disproportionately contribute to GHGs fluxes, informing policies that can be designed to minimize GHGs emissions. More artificial and natural lakes GHG data covering detailed spatial and temporal dynamics are required for more accurate assessments of regional and global emissions. New datasets should include not only reservoir water surfaces, but also turbines, spillways and rivers downstream of dams.

## Competing financial interests

The authors declare no competing financial interests.

## Author contributions

SYL designed the study, mined data and carried out all computations, data analysis, data interpretation, and drafted the manuscript. All the authors contributed to manuscript writing and discussion.

## Acknowledgements

This research was funded by the National Natural Science Foundation of China (No. 31670473) and 'Hundred-talent Program' of the Chinese Academy of Sciences (R53A362Z10) that were granted to Li, Australian Research Council (FT170100327) to Santos, and National University of Singapore HSS grant (R-109-000-172-646) to Lu. We acknowledge the helpful input provided by David Bastviken and Jonathan Cole, and Paul Macklin for drawing Fig. 1. We thanked the editor and anonymous reviewers for the constructive comments to improve the paper.

## Appendix A. Supplementary data

Supplementary data to this article can be found online at https://doi.org/10.1016/j.watres.2018.09.053.

## References


Abril, G., Bouillon, S., Darchambeau, F., Teodoru, C.R., Marwick, T.R., Tamooh, F., Omengo, F.O., Geeraert, N., Deirmendjian, L., Polsenaere, P., Borges, A.V., 2015. Technical Note: large overestimation of pCO(2) calculated from pH and alkalinity in acidic, organic-rich freshwaters. Biogeosciences 12, 67–78.

Aufdenkampe, A.K., Mayorga, E., Raymond, P.A., Melack, J.M., Doney, S.C., Alin, S.R., Aalto, R.E., Yoo, K., 2011. Riverine coupling of biogeochemical cycles between land, oceans, and atmosphere. Front. Ecol. Environ. 9, 53–60.

Baron, J.S., Hall, E.K., Nolan, B.T., Finlay, J.C., Bernhardt, E.S., Harrison, J.A., Chan, F., Boyer, E.W., 2013. The interactive effects of excess reactive nitrogen and climate change on aquatic ecosystems and water resources of the United States. Biogeochemistry 114, 71–92.

Barros, N., Cole, J.J., Tranvik, L.J., Prairie, Y.T., Bastviken, D., Huszar, V.L.M., Giorgio, P.D., Roland, F., 2011. Carbon emission from hydroelectric reservoirs linked to reservoir age and latitude. Nat. Geosci. 4, 593–596.

Bastviken, D., Cole, J., Pace, M., Tranvik, L., 2004. Methane emissions from lakes: dependence of lake characteristics, two regional assessments, and a global estimate. Global Biogeochem. Cycles 18.

Bastviken, D., Tranvik, L.J., Downing, J.A., Crill, P.M., Enrichprast, A., 2011. Freshwater methane emissions offset the continental carbon sink. Science 331, 50-50.

Chen, H., Zhu, Q.A., Peng, C.H., Wu, N., Wang, Y.F., Fang, X.Q., Jiang, H., Xiang, W.H., Chang, J., Deng, X.W., Yu, G.R., 2013. Methane emissions from rice paddies natural wetlands, lakes in China: synthesis new estimate. Global Change Biol. 19, 19–32.

Chrzanowski, T.H., Grover, J.P., 2001. The light: nutrient ratio in lakes: a test of hypothesized trends in bacterial nutrient limitation. Ecol. Lett. 4, 453–457.

Chu, Z.X., Zhai, S.K., Lu, X.X., Liu, J.P., Xu, J.X., Xu, K.H., 2009. A quantitative assessment of human impacts on decrease in sediment flux from major Chinese rivers entering the western Pacific Ocean. Geophys. Res. Lett. 36.

Cole, J.J., Prairie, Y.T., Caraco, N.F., McDowell, W.H., Tranvik, L.J., Striegl, R.G., Duarte, C.M., Kortelainen, P., Downing, J.A., Middelburg, J.J., Melack, J., 2007. Plumbing the global carbon cycle: integrating inland waters into the terrestrial carbon budget. Ecosystems 10, 172–185.

Deemer, B.R., Harrison, J.A., Li, S., Beaulieu, J.J., Delsontro, T., Barros, N., Bezerra-Neto, J.F., Powers, S.M., dos Santos, M.A., Vonk, J.A., 2016. Greenhouse gas emissions from reservoir water surfaces: a new global synthesis. Bioscience 66, 949–964.

DelSontro, T., Beaulieu, J.J., Downing, J.A., 2018. Greenhouse gas emissions from lakes and impoundments: upscaling in the face of global change. Limnology and Oceanography Letters 3, 64–75.

DelSontro, T., Kunz, M.J., Kempter, T., Wuest, A., Wehrli, B., Senn, D.B., 2011. Spatial heterogeneity of methane ebullition in a large tropical reservoir. Environ. Sci. Technol. 45, 9866–9873.

dos Santos, M.A., Rosa, L.P., Sikar, B., Sikar, E., dos Santos, E.O., 2006. Gross greenhouse gas fluxes from hydro-power reservoir compared to thermo-power plants. Energy Pol. 34, 481–488.

Downing, J.A., Cole, J.J., Duarte, C.M., Middelburg, J.J., Melack, J.M., Prairie, Y.T., Kortelainen, P., Striegl, R.G., McDowell, W.H., Tranvik, L.J., 2012. Global abundance and size distribution of streams and rivers. Inland Waters 2, 229–236.

Downing, J.A., Prairie, Y.T., Cole, J.J., Duarte, C.M., Tranvik, L.J., Striegl, R.G., Mcdowell, W.H., Kortelainen, P., Caraco, N.F., Melack, J.M., 2006. The global abundance and size distribution of lakes, ponds, and impoundments. Encyclopedia of Inland Waters 51, 469–478.

Fearnside, P.M., 2005. Do hydroelectric dams mitigate global warming? The case of Brazil's CuruÁ-una dam. Mitig. Adapt. Strategies Glob. Change 10, 675–691.

Fearnside, P.M., Pueyo, S., 2012. COMMENTARY: greenhouse-gas emissions from tropical dams. Nat. Clim. Change 2, 382–384.

Giles, J., 2006. Methane quashes green credentials of hydropower. Nature 444, 524–525.

Gudasz, C., Bastviken, D., Steger, K., Premke, K., Sobek, S., Tranvik, L.J., 2010. Temperature-controlled organic carbon mineralization in lake sediments. Nature 466, 1134.

Guerin, F., Abril, G., Richard, S., Burban, B., Reynouard, C., Seyler, P., Delmas, R., 2006. Methane and carbon dioxide emissions from tropical reservoirs: significance of downstream rivers. Geophys. Res. Lett. 33.

Halbedel, S., Koschorreck, M., 2013. Regulation of CO2 emissions from temperate streams and reservoirs. Biogeosciences 10, 7539–7551.

Hertwich, E.G., 2013. Addressing biogenic greenhouse gas emissions from hydropower in LCA. Environ. Sci. Technol. 47, 9604–9611.

Holgerson, M.A., Raymond, P.A., 2016. Large contribution to inland water CO2 and CH4 emissions from very small ponds. Nat. Geosci. 9, 222-U150.

Humborg, C., Morth, C.M., Sundbom, M., Borg, H., Blenckner, T., Giesler, R., Ittekkot, V., 2010. CO2 supersaturation along the aquatic conduit in Swedish watersheds as constrained by terrestrial respiration, aquatic respiration and weathering. Global Change Biol. 16, 1966–1978.

Kemenes, A., Forsberg, B.R., Melack, J.M., 2007. Methane release below a tropical hydroelectric dam. Geophys. Res. Lett. 34.

Kemenes, A., Forsberg, B.R., Melack, J.M., 2011. $CO_2$ emissions from a tropical hydroelectric reservoir (Balbina, Brazil). Journal of Geophysical Research-Biogeosciences 116.

Knoll, L.B., Vanni, M.J., Renwick, W.H., Dittman, E.K., Gephart, J.A., 2013. Temperate reservoirs are large carbon sinks and small CO2 sources: results from high-resolution carbon budgets. Global Biogeochem. Cycles 27, 52–64.

Krist, A.C., Kay, A.D., Scherber, E., Larkin, K., Brown, B.J., Lu, D.N., Warren, D.T., Riedl, R., Neiman, M., 2016. Evidence for extensive but variable nutrient limitation in New Zealand lakes. Evol. Ecol. 30, 973–990.

Li, S., Bush, R.T., 2015. Revision of methane and carbon dioxide emissions from inland waters in India. Global Change Biol. 21, 6–8.

Li, S., Zhang, Q., 2014a. Carbon emission from global hydroelectric reservoirs revisited. Environ. Sci. Pollut. Res. Int. 21, 13636–13641.

Li, S., Zhang, Q., 2014b. Partial pressure of CO2 and CO2 emission in a monsoon-driven hydroelectric reservoir (Danjiangkou Reservoir), China. Ecol. Eng. 71, 401–414.

Lu, X.X., Li, S., He, M., Zhou, Y., Li, L., Ziegler, A.D., 2012. Organic carbon fluxes from the upper Yangtze basin: an example of the Longchuanjiang River, China. Hydrol. Process. 26, 1604–1616.

Ma, R.H., Yang, G.S., Duan, H.T., Jiang, J.H., Wang, S.M., Feng, X.Z., Li, A.N., Kong, F.X., Xue, B., Wu, J.L., Li, S.J., 2011. China's lakes at present: number, area and spatial distribution. Sci. China Earth Sci. 54, 283–289.

Marotta, H., Pinho, L., Gudasz, C., Bastviken, D., Tranvik, L.J., Enrichprast, A., 2014. Greenhouse gas production in low-latitude lake sediments responds strongly to warming. Nat. Clim. Change 4, 467–470.

Mayorga, E., Aufdenkampe, A.K., Masiello, C.A., Krusche, A.V., Hedges, J.I., Quay, P.D., Richey, J.E., Brown, T.A., 2005. Young organic matter as a source of carbon dioxide outgassing from Amazonian rivers. Nature 436, 538–541.

MWR, 2016. (Ministry of Water Resources in China). China Water Statistical Yearbook. China Water Power Press, Beijing.

Myhre, G., Shindell, D., Bréon, F.M., Collins, W., Fuglestvedt, J., Huang, J., Koch, D., Lamarque, J.F., Lee, D., Mendoza, B., Nakajima, T., Robock, A., Stephens, G., Takemura, T., Zhang, H., 2013. Anthropogenic and natural radiative forcing. Retrieved from. In: Climate Change 2013: the Physical Science Basis. Contribution of Working Group I to the Fifth Assessment Report of the

Intergovernmental Panel on Climate Change (Cambridge, United Kingdom and New York, NY, USA).
NEA, 2016. (National Energy Administration of China). "13rd Five-year" Plan for Hydropower Development.
Piao, S.L., Fang, J.Y., Ciais, P., Peylin, P., Huang, Y., Sitch, S., Wang, T., 2009. The carbon balance of terrestrial ecosystems in China. Nature 458, 1009–U1082.
Prairie, Y.T., Alm, J., Beaulieu, J., Barros, N., Battin, T., Cole, J., del Giorgio, P., DelSontro, T., Guérin, F., Harby, A., Harrison, J., Mercier-Blais, S., Serça, D., Sobek, S., Vachon, D., 2017. Greenhouse Gas Emissions from Freshwater Reservoirs: what Does the Atmosphere See? Ecosystems.
Rantakari, M., Kortelainen, P., 2005. Interannual variation and climatic regulation of the CO2 emission from large boreal lakes. Global Change Biol. 11, 1368–1380.
Rantakari, M., Kortelainen, P., 2008. Controls of organic and inorganic carbon in randomly selected Boreal lakes in varied catchments. Biogeochemistry 91, 151–162.
Raymond, P.A., Hartmann, J., Lauerwald, R., Sobek, S., McDonald, C., Hoover, M., Butman, D., Striegl, R., Mayorga, E., Humborg, C., Kortelainen, P., Durr, H., Meybeck, M., Ciais, P., Guth, P., 2013. Global carbon dioxide emissions from inland waters. Nature 503, 355–359.
Roehm, C., Tremblay, A., 2006. Role of turbines in the carbon dioxide emissions from two boreal reservoirs, Quebec, Canada. Journal of Geophysical Research-Atmospheres 111.
St Louis, V.L., Kelly, C.A., Duchemin, E., Rudd, J.W.M., Rosenberg, D.M., 2000. Reservoir surfaces as sources of greenhouse gases to the atmosphere: a global estimate. Bioscience 50, 766–775.
Teodoru, C.R., Del Giorgio, P.A., Prairie, Y.T., Camire, M., 2009. Patterns in pCO(2) in boreal streams and rivers of northern Quebec, Canada. Global Biogeochem. Cycles 23, 11.
Teodoru, C.R., Nyoni, F.C., Borges, A.V., Darchambeau, F., Nyambe, I., Bouillon, S., 2015. Dynamics of greenhouse gases ($CO_2$, $CH_4$, $N_2O$) along the Zambezi River and major tributaries, and their importance in the riverine carbon budget. Biogeosciences 12, 2431–2453.
Tian, H., Melillo, J., Lu, C., Kicklighter, D., Liu, M., Ren, W., Xu, X., Chen, G., Zhang, C., Pan, S., Liu, J., Running, S., 2011. China's terrestrial carbon balance: contributions from multiple global change factors. Global Biogeochem. Cycles 25.
Tranvik, L.J., Downing, J.A., Cotner, J.B., Loiselle, S.A., Striegl, R.G., Ballatore, T.J., Dillon, P., Finlay, K., Fortino, K., Knoll, L.B., 2009. Lakes and reservoirs as regulators of carbon cycling and climate. Limnol. Oceanogr. 54, 2298–2314.
Verpoorter, C., Kutser, T., Seekell, D.A., Tranvik, L.J., 2014. A global inventory of lakes based on high-resolution satellite imagery. Geophys. Res. Lett. 41, 6396–6402.
Vrede, K., 2005. Nutrient and temperature limitation of bacterioplankton growth in temperate lakes. Microb. Ecol. 49, 245–256.
Wang, C.H., Xiao, S.B., Li, Y.C., Zhong, H.Y., Li, X.C., Peng, F., 2014. Methane formation and consumption processes in Xiangxi Bay of the three gorges reservoir. Sci. Rep. 4.
Wang, F., Wang, Y., Zhang, J., Xu, H., Wei, X., 2007. Human impact on the historical change of CO2 degassing flux in River Changjiang. Geochem. Trans. 8.
Xiao, S.B., Liu, D.F., Wang, Y.C., Yang, Z.J., Chen, W.Z., 2013. Temporal variation of methane flux from Xiangxi Bay of the three gorges reservoir. Sci. Rep. 3.
Yang, H., Xie, P., Ni, L., Flower, R.J., 2011a. Underestimation of CH4 emission from freshwater lakes in China. Environ. Sci. Technol. 45, 4203–4204.
Yang, M., Li, H.L., Lei, T., Zhou, Y., Lu, C., Li, L., Lei, G.C., Wang, J.S., Lu, X.G., 2011b. Spatial-temporal characteristics of methane emission flux and its influence factors at miyun reservoir in Beijing. Wetland Science 9, 191–197.
Yang, X., Lu, X., 2013. Drastic change in China's lakes and reservoirs over the past decades. Sci. Rep. 4, 6041-6041.
Zarfl, C., Lumsdon, A.E., Berlekamp, J., Tydecks, L., Tockner, K., 2015. A global boom in hydropower dam construction. Aquat. Sci. 77, 161–170.
Zheng, H., Zhao, X., Zhao, T., Chen, F., Xu, W., Duan, X., Wang, X., Ouyang, Z., 2011. Spatial-temporal variations of methane emissions from the Ertan hydroelectric reservoir in southwest China. Hydrol. Process. 25, 1391–1396.
Zhu, D., Wu, Y., Chen, H., He, Y., Wu, N., 2016. Intense methane ebullition from open water area of a shallow peatland lake on the eastern Tibetan Plateau. Sci. Total Environ. 542, 57–64.